Journal of Nuclear Materials 438 (2013) 116–125

Contents lists available at SciVerse ScienceDirect

Journal of Nuclear Materials

journal homepage: www.elsevier.com/locate/jnucmat

Corrosion of steel drums containing cemented ion-exchange resins as intermediate level nuclear waste

G.S. Duffó [a,b,c], S.B. Farina [a,b,c,*], F.M. Schulz [c]

[a] Departamento de Materiales, Comisión Nacional de Energía Atómica, Av. Gral. Paz 1499, 1650 Buenos Aires, Argentina
[b] Universidad Nacional de San Martín, Av. Gral. Paz 1499, 1650 Buenos Aires, Argentina
[c] Consejo Nacional de Investigaciones Científicas y Tecnológicas – CONICET, Av. Gral. Paz 1499, 1650 Buenos Aires, Argentina

HIGHLIGHTS

- There are no works related to the corrosion of drums containing radioactive waste.
- Chloride induces high corrosion rate and after 1 year it drops abruptly.
- Decrease in the corrosion rate is due to the lack of water to sustain the process.
- Cementated ion-exchange resins do not pose risks of corrosion of the steel drums.

ARTICLE INFO

Article history:
Received 18 December 2012
Accepted 4 March 2013
Available online 21 March 2013

ABSTRACT

Exhausted ion-exchange resins used in nuclear reactors are immobilized by cementation before being stored. They are contained in steel drums that may undergo internal corrosion depending on the presence of certain contaminants. The objective of this work is to evaluate the corrosion susceptibility of steel drums in contact with cemented ion-exchange resins with different aggressive species. The corrosion potential and the corrosion rate of the steel, and the electrical resistivity of the matrix were monitored for 900 days. Results show that the cementation of ion-exchange resins seems not to pose special risks regarding the corrosion of the steel drums.

1. Introduction

The radioactive waste is classified according to its radioactivity level, half-life and disposal technology, and in the Argentine Republic, the National Radioactive Waste Management Programme is responsible for evaluating and developing different alternatives for its final disposal [1]. In the case of Intermediate Level Radioactive Waste (ILW), the proposed model is the near-surface monolithic repository similar to those in operation in L. Aube, France and El Cabril, Spain. The design of this type of repository is based on the use of multiple, redundant and independent barriers. These barriers include: waste forms and metallic disposal containers (waste will be immobilized in cement matrices and packed in 200 l drums or in special concrete containers), backfill and buffer materials, vaults and cover and geological media. The model foresees a period of 300 years of institutional post-closure control. Intermediate level radioactive solid wastes originated in the operation and maintenance activities of the two nuclear power plants operating in Argentina, consist mainly of mechanical filters from the primary circuit of the reactor and of spent ion-exchange resin beds. Such intermediate level radioactive solid waste is stored at the facilities of each power plant awaiting treatment and conditioning.

Treatment of these wastes is necessary for long term storage and disposal. For this purpose, different methods are employed to immobilize the radioactive wastes in a solidified form: solidification, embedding or encapsulation [2].

Intermediate and low level radioactive wastes – i.e., those that generate little or no heat during storage – are usually immobilized in cement, within steel drums, prior to interim storage and eventual disposal. Cements are capable of immobilizing wastes, even powder or flocculated ones, producing waste forms that provide mechanical support as well as a chemical environment which tends to bind metallic ions very well, as hydroxide bound species, with very low mobility. Besides, cement is favoured as it is readily available, has low cost, has controllable diffusion characteristics and acts as radiation shielding. Portland cement grout is normally used, combined with slow-reacting pozzolans to reduce both the heat generated during hydration and the eventual permeability. However, cementation has two main limits: the volume increase generated by the conditioning process and the possible adverse cement-waste interaction. The use of cementitious encapsulants

* Corresponding author at: Departamento de Materiales, Comisión Nacional de Energía Atómica, Av. Gral. Paz 1499, 1650 Buenos Aires, Argentina. Tel.: +54 11 6772 7403; fax: +54 11 6772 7388.
E-mail address: farina@cnea.gov.ar (S.B. Farina).

0022-3115/$ - see front matter © 2013 Elsevier B.V. All rights reserved.
http://dx.doi.org/10.1016/j.jnucmat.2013.03.027

to immobilize waste materials in the nuclear industry is a well established procedure to produce durable and safe wasteforms. The direct encapsulation of ILW in cement started back in 1982 by British Nuclear Fuels Limited (BNFL) when this disposal strategy was adopted for wastes arising from the reprocessing of spent nuclear fuel [3].

Ion-exchange resins are one of the most common and effective treatment methods to decontaminate liquid radioactive waste. It is a well-developed technique that has been employed for many years in the nuclear industry as well as in other industries. However, spent ion-exchange resins are considered to be problematic waste that in many cases requires special approaches and precautions during its immobilization to meet the acceptance criteria for disposal [4].

Immobilization of spent ion-exchange resins by a cementation process is frequently used for economical reasons as well as for being a simple operation [5–7], although direct immobilization of spent resins into cementitious materials had some drawback such as no volume reduction and relatively high leachability. This is why other forms of immobilization such as bituminization and polymer encapsulation are also used [8]. For ion-exchange resins cementation, the main research focuses on increasing the loading of spent resins, reducing leaching of radionuclides, improving the compression strength of the matrix and controlling the heat generated by exothermic hydration reactions during cementation. As a consequence of this research, some new developments of cement solidification have appeared in the last few years [9–11].

After immobilization, ion-exchange resins are conditioned in steel drums that, in turn, may undergo internal corrosion depending on the presence of certain contaminants in the waste. An extra enclosure made of concrete is required to guarantee the radionuclides containment. As a consequence of a conservative approach to the safety analysis, the steel drums are not considered to be physical barriers, with the concrete assumed to be the sole barrier to prevent radionuclide release during the lifespan of the facility. However, if the durability of the steel drums could be guaranteed, an extra security period could be claimed.

This work describes the study of the corrosion susceptibility of the inner wall of steel drums in contact with cemented ion-exchange resins contaminated with different types and concentrations of aggressive species. To achieve this aim, a special type of specimen was manufactured to simulate the cemented ion-exchange resins in the drum [12]. The evolution of the corrosion potential and the corrosion rate of the steel, as well as the electrical resistivity of the matrix were monitored over a period of 900 days. The aggressive species studied were chloride ions (the main ionic species of concern that could be found within the ionic-exchange resins); and sulphate ions (produced during radiolysis of the cationic exchange-resins after cementation [13]). The work was complemented with an analysis of the corrosion products formed on the steel in each condition, as well as the morphology of the corrosion process.

2. Experimental techniques

The specimens used in the present study were manufactured to simulate cemented ion-exchange resins in the drums (Fig. 1). Each specimen consists of a sheet of the steel used to manufacture the drums (0.9 mm in thick), $6 \times 6\ cm^2$ in area, and a PVC tube (4.5 cm in diameter and 7.0 cm in height) attached to the steel sheet by a two-component epoxy putty used for sanitary repairs. The chemical composition of the steel is as follows (wt.%): C, 0.069%; Si, 0.08%; Mn, 0.43%; P, 0.009%, S, 0.005%, Fe, balance. This composition corresponds to a steel SAE 1006. The steel drums are usually painted both inside and outside, though in this study the steel was used with no coating.

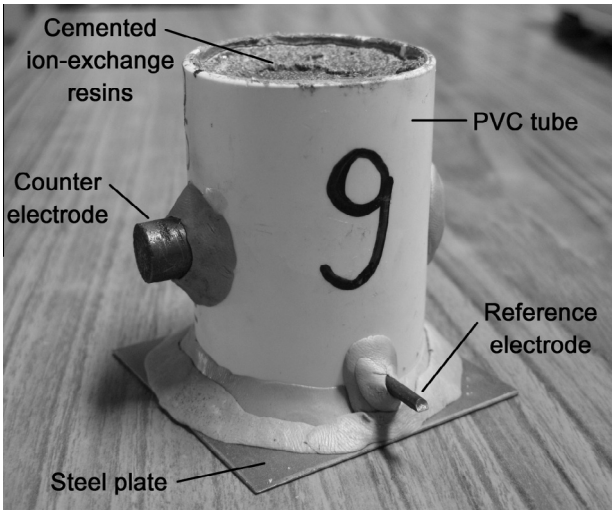

Fig. 1. Specimen manufactured to simulate the cemented ion-exchange resins in the steel drums, before covering with a PVC lid.

When working in cementitious materials special reference electrodes are required. In general, a good reference electrode must have a stable potential along time, in spite of changes in temperature and moisture; but, in the particular case of an embedded electrode, it must also be rugged and reasonably small and unobtrusive to allow easy placement in a structure. Then, typical reference electrodes such as saturated calomel electrodes have to be disregarded as they are not appropriate for embedding in concrete due to their glass body. Solid reference electrodes are mandatory for this purpose. In the present work, a graphite bar, 1.2 cm in diameter, was used as counter electrode, and a titanium bar activated with mixed-metal oxide (MMO) was used as reference electrode. This type of electrodes are made from activated titanium rods produced commercially for permanent impressed-current anodes in cathodic protection of reinforcing steel in concrete. The surface of the titanium rod is covered with a precious mixed-metal oxide applied using a proprietary process (WWI Procat, S.L., Spain). MMO electrodes are widely used and the behaviour of this type of reference electrode in concrete was previously studied [14,15]. Both electrodes were placed inside the PVC tube as shown in Fig. 1. The counterelectrode passes through the tube while the reference electrode reaches the centre of the tube. After sealing with the putty, the cemented waste forms, prepared as described below, were placed inside the tube. Finally, a PVC lid was put on the tube in order to avoid the access of oxygen to the specimen. The specimens, so prepared, were left exposed to laboratory conditions, where the temperature is 24.1 ± 2.9 °C.

The simulation of exhausted ion-exchange resins was made by mixing Cationic Resin Lewatit® S100 KR/H+ and Anionic Resin Lewatit® M500 KR/OH- of Bayer Chemicals, in a proportion equal to 1.137 (in weight) with an aqueous solution containing 15% w/w of $NaNO_3$ and 3.7% w/w of NaOH (both analytical grade). In this way, the quantity of anions and cations present in solution is enough for complete saturation of the resins. The general properties of the resins used in this work are shown in Table 1. After a 24-h saturation period (stirring periodically), the supernatant liquid was removed and the resins were rinsed 5 times with ultra pure water. The resulting product was mixed with cement (Ordinary Portland Cement CPN 40 ARS, Loma Negra®) and water, according to standards ASTM C-305 and AASHTO T-162 for the preparation of mortars. The composition of the cement used is shown in Table 2. The final mix has the following composition: ion-exchange resins (by weight of dry components), 14.2%; cement, 56.8% and water.

Table 1
General properties of the ion-exchange resins used in the present work.

Name	Lewatit® MonoPlus S 100 KR	Lewatit® MonoPlus M 500 KR
Classification	Cationic strong acid	Anionic strong base
Ionic form	H^+	OH^-
Functional group	Sulfonic acid	Quaternary amine, type I
Matrix	Crosslinked polystyrene	Crosslinked polystyrene
Structure	Gel type beds	Gel type beds
Mean bead size (mm)	0.62 (±0.05)	0.64 (±0.05)
Density dry (g/ml)	1.22	1.08
Bulk density wet (g/L)	780	650
Exchange capacity (eq/ml)	1.8	1.0
Water retention (wt.%)	47/53	65/75

The final formulation has a water/cement (w/c) ratio equal to 0.51. This mix is then placed inside the PVC tubes.

To evaluate the corrosion resistance of the steel under different aggressive conditions, four different sets of specimens were prepared. Each set consists of 6 specimens. Then, a total of 24 specimens, 6 for each condition, were made. The first set contains no aggressive species in the formulation. The second and third sets contain NaCl added to the mix in two proportions: 0.5 wt.% and 5 wt.% of chloride ions with respect to the cement weight, respectively. The fourth set contains Na_2SO_4 at a concentration of 2.3 wt.% of sulphate with respect to the cement weight. The addition of chloride and sulphate ions was made by adding the respective salts (NaCl and Na_2SO_4) to the water used to prepare the final mix. The introduction of sulphate ions represents the situation in which cationic resins, that have sulphonic groups in their structure, are damaged by radiolysis and release sulphate ions to the system. The sulphate concentration used in the present work represents the maximum quantity of sulphate ions that can be released under γ-radiation, and corresponds to 33% degradation of pure cationic resins [13]. In addition, prismatic specimens were prepared for mechanical tests and microscopic observations. The mechanical properties of the matrix obtained were: compressive strength 18.9 ± 2.2 MPa, and flexural strength 4.4 ± 0.8 MPa.

The electrochemical parameters normally used to characterise the corrosion behaviour of steel in contact with cementitious materials were monitored periodically: the electrical resistivity of the cemented waste forms (ρ) determined from resistance measurements between the steel sheet and the MMO reference electrode; the corrosion potential (Ecorr) of the steel measured against the MMO reference electrode and the corrosion rate of the steel (CR) obtained from the linear polarisation resistance (Rp) technique and the application of the Stern–Geary relationship [16]. The electrical resistivity of the matrix was measured by applying a sinusoidal signal ($\Delta V = 10$ mV, $\nu = 10$ kHz) between the steel sheet and the internal reference electrode, and computing the value of the resistance from the ratio between the peak voltage and the peak current. In order to determine the electrical resistivity, the device was calibrated with KCl solutions (ranging from 10^{-5} to 1 M) of known resistivity. Besides, when computing the corrosion current density (and hence, the corrosion rate), a correction for ohmic drop was performed based on the resistance measurements made between the steel sheet and the MMO reference electrode. Repetitive results were obtained in all cases and, for the sake of simplicity, only representative values are reported in the results section. The potentials are reported versus the copper/saturated copper sulphate reference electrode scale (CSE) according to a previously determined relationship [14,15] ($E_{V(CSE)} = E_{V(MOM)} - 0.120$ V).

After 900 days of testing, the steel sheets were broken apart from the specimens and observed with both, optical (Olympus BX60M) and scanning electron microscope (SEM, Quanta 200). Energy Dispersion X-ray analysis (EDAX) was performed at many locations of the steel sheet and in the cementitious matrix to assess the local chemical composition. After removing the rust scale in a 10% ammonium citrate solution at 60 °C (descaling), the steel sheets were observed again under the SEM. Metallographic cross sections of both, non-descaled and descaled specimens were prepared by cutting small pieces of the sheets, and mounting them in curing epoxy at room temperature. The mounted specimens were grounded with emery papers (grades 220–600) and then polished with a diamond paste and observed with both, optical and SEM, in order to determine the morphology as well as the depth of the corrosive attack. Additionally, corrosion products were analysed by Transmission Mössbauer Spectroscopy (TMS). In this case, the analysis was performed using a ^{57}Co source in a Rh matrix. To identify the compounds, TMS of the corrosion products was performed at room temperature (RT). Analysis of the spectra was performed using the Normos least-squares fitting program [17]. Isomer shift values are given relative to α-Fe at room temperature.

Table 2
Composition of the cement used (g/100 g).

Compound	%
SiO_2	21.4
CaO	64.5
Al_2O_3	3.46
Fe_2O_3	4.90
SO_3	2.04
MgO	0.82
Na_2O	0.07
K_2O	0.93
Cl^-	<0.01
S^{2-}	<0.01

3. Results and discussion

Fig. 2 shows a scanning electron micrograph of the resins solidified in the cement matrix. The resins and cement had not solidified together. The resin particles are only physically encapsulated rather than fully bonded, and this is why some resin particles have dropped from the cement matrix leaving holes.

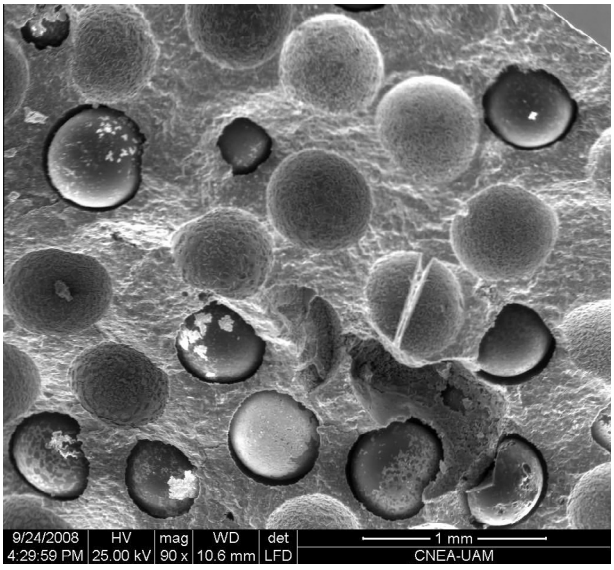

Fig. 2. Scanning electron micrograph of ion-exchange resins encapsulated in a cement matrix.

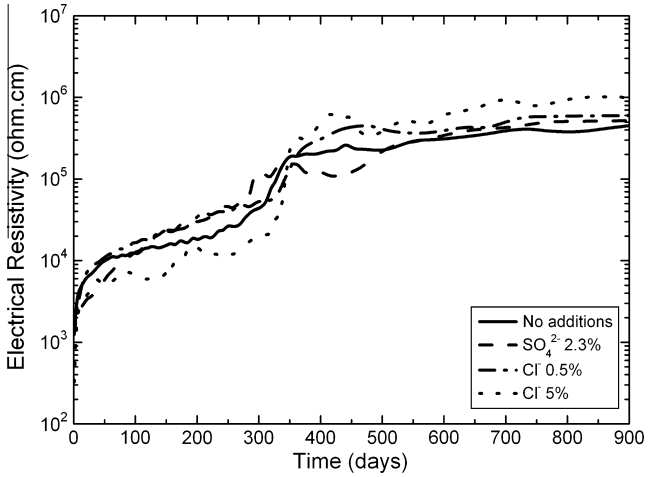

Fig. 3. Matrix electrical resistivity as a function of time for the tested formulations (compositions are expressed as wt.% with respect to the cement weight).

Results were repetitive and for the sake of simplicity only a representative value is shown in the following figures. Fig. 3 shows the matrix electrical resistivity as a function of time. The matrix electrical resistivity has a tendency to increase with time, which reflects the continuous hydration process showed by the system. Although the increase in the resistivity is continuous, there are two changes in the slope at about 300 and 400 days of exposure. In all cases, at the end of the tests (900 days), the values of the electrical resistivity lie between 500 and 1000 kohm cm. These values, according to Andrade and Alonso [18], imply negligible corrosion because the matrix is too dry. The addition of chloride ions and sulphate ions seems to have little effect on the electrical resistivity after a long period of exposition.

Fig. 4 shows the evolution of the corrosion potential of the steel plates as a function of time. In the case of no additions to the mix, the potential remains stable during the 900 days of exposure, with a value close to $-0.120\ V_{CSE}$. The same behaviour is found when sulphate ions are added. Additions of 0.5 wt.% chloride ions shift the corrosion potential towards more negative values (close to $-0.320\ V_{CSE}$) after an induction time of approximately 30 days. After about 300 days, the corrosion potential increases monotonously and at 900 days reaches a value close to those obtained with no contaminant additions or with the addition of sulphate ions. Finally, specimens with the addition of 5 wt.% chloride show a corrosion potential close to $-0.520\ V_{CSE}$ immediately after the start of the test. This value remains almost constant for 250 days and afterwards increases slowly reaching a value of $-0.270\ V_{CSE}$ after 900 days of exposure.

Even though a lid was put on the PVC tubes in order to simulate in the laboratory the waste forms inside the drums as much as possible, there was enough oxygen inside the specimens to sustain the cathodic reaction of oxygen. This oxygen supply came from the oxygen dissolved in the water used to prepared the mix, as well as from the exchange resins. Thus, the corrosion process of the steel sheet is the result of the oxidation of the metal (anodic process) and the reduction of oxygen (cathodic process). According to ASTM C-0876 standard [19], steel plates in contact with non-contaminated matrix or with the addition of sulphate ions are in a passive state (corrosion potential higher than $-0.2\ V_{CSE}$) with a very low corrosion probability (<5%). On the other hand, steel plates in contact with a matrix highly contaminated with chloride (5 wt.%), are in the active state (corrosion potential lower than $-0.35\ V_{CSE}$) from the beginning of the test up to about 350 days, with a very high corrosion probability (>95%). Then, the corrosion potential increases reaching values at which, according to the standard, the probability of corrosion is uncertain (corrosion potentials between $-0.35\ V_{CSE}$ and $-0.2\ V_{CSE}$). Finally, in the presence of 0.5 wt.% chloride ion concentration, the probability of corrosion is uncertain from the beginning of the test up to about 400 days, when the steel plates passivate.

Fig. 5 shows the corrosion rate of steel as a function of time. Corrosion rates were calculated using the expression $CR = k \cdot B/Rp$ where B is a constant that depends on the active/passive state of the steel: B is equal to 0.026 V, in the case the steel is in the active state, and 0.052 V in the case of passive state [20]. k is a constant that relates corrosion current densities and corrosion rates by applying Faradaýs Law [$k = 11.6$ (μm/year)/(μA/cm^2)].

In the case of formulations with no additions, or with the addition of sulphate, the CR slowly decreases from less than 1 μm/year to about 0.01 μm/year. These values are consistent with the values of the corrosion potential that indicate a passive state of the steel. On the other hand, in matrixes with additions of 0.5 wt.% chloride ions, the CR increases with time during the first 100 days to reach a value close to 10 μm/year, and then slowly decreases reaching a value of 0.4 μm/year after 900 days of exposure. Finally, for 5 wt.% chloride addition, the CR value shows a sharp increase during the first 300 days reaching a value close to 1 mm/year.

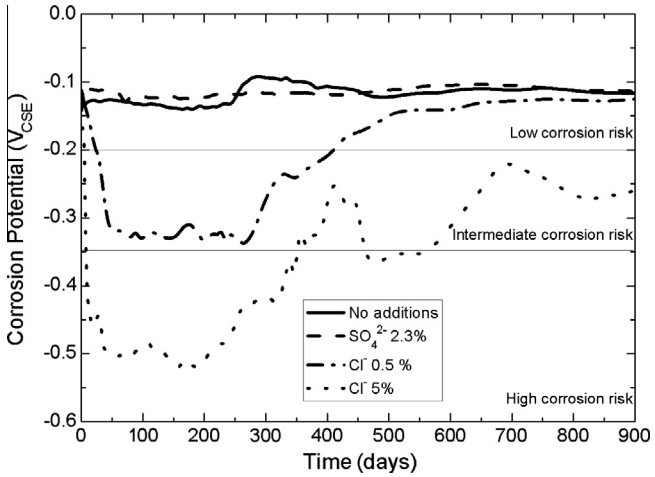

Fig. 4. Corrosion potential as a function of time for the tested formulations (compositions are expressed as wt.% with respect to the cement weight).

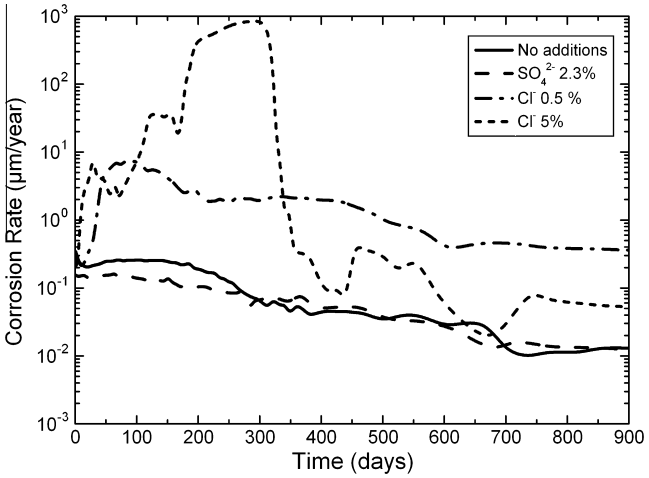

Fig. 5. Corrosion rate as a function of time for the tested formulations (compositions are expressed as wt.% with respect to the cement weight).

Afterwards, the CR starts to decrease monotonically reaching, at the end of the test, a CR value close to those obtained in matrixes with no additions, or with the additions of sulphate ions. To sum up, in all cases, after 900 days, the steel plates behave as if they were passivated (no matter the additions of aggressive species) with a low or negligible CR [21].

It can be seen that there is a good correlation between the qualitative predictions of the ASTM C-0876 standard [19] and the corrosion rates measured with the linear polarisation resistance technique: the higher the corrosion potential (and hence the lower the corrosion probability according to the ASTM standard), the lower the corrosion rate measured. This leads to the conclusion that ASTM C-0876 standard [19], originally developed for the qualitative determination of the state of steel bars embedded in concrete (reinforced concrete), can also be applied straightforward in systems like those studied in the present work.

After finishing the tests, specimens were broken apart to observe the condition of the steel plates. Fig. 6a–d shows macrographs of the steel plates exposed to different formulations. It can be seen that, while specimens in contact with a matrix with no additions or with additions of 2.3 wt.% sulphate (Fig. 6a and b) show little evidence of corrosion, steel plates in contact with a matrix contaminated with chloride appear to be highly corroded and covered with corrosion products (Fig. 6c and d). The higher the chloride content, the larger the amount of corrosion products. The corrosion products are black, red, brown and orange, and in all cases they are extremely dry. The rust layer is heterogeneous and irregular, and the depth of the corrosion product layer is larger in the most concentrated chloride conditions. In the more diluted chloride conditions, some spots without corrosive attack can be seen in Fig. 6c. According to the literature, the reddish corrosion products are ordinary rust that generally contains lepidocrocite and/or akaganeite.

The plates were observed under the SEM and Figs. 7–9 show the micrographs obtained. Fig. 7a and b correspond to specimens with no additions and the addition of 2.3 wt.% sulphate, respectively. It can be observed that, in both cases, the steel shows white products, that are remains of the cementitious matrix (determined by EDAX), with no corrosion products.

Fig. 8 shows the steel plate of the specimens with the addition of 0.5 wt.% chloride. Corrosion products are observed with low magnification (Fig. 8a). Higher magnification (Fig. 8b) reveals the presence of corrosion products of different morphologies: compact corrosion products showing cracks, grown over crystals showing fine plates (“flowery” structures), probably due to lepidocrocite (γ-FeOOH).

Fig. 9 shows the steel plate of the specimens with the addition of 5 wt.% chloride. At low magnification (Fig. 9a), corrosion products of different morphologies can be observed. Fig. 9b shows needle-like crystals corresponding to whiskers of goethite (α-FeOOH). Fig. 9c shows a globular (“cotton-ball”) pattern, typical of akaganeite (β-FeOOH). In Fig. 9d, a first formed amorphous layer appears as a sedimentary soil layer in which cracks develop during drying. On top of this layer, circular grains showing bulges appear as donuts, corresponding to magnetite (Fe_3O_4). The assignment of these crystal structures was based on the comparison between the morphologies of the corrosion products observed in the present work with those reported in earlier works [22–25].

Fig. 10 shows the steel plates exposed to different matrixes, after descaling with 10% ammonium citrate solutions. Fig. 10a corresponds to a specimen exposed to a matrix with no additions. It can be observed that no corrosion attack has occurred (the descaling reagent has eliminated the remains of the cementitious matrix observed in Fig. 7a). Similar results were obtained with steel plates exposed to sulphate (not shown). Fig. 10b shows the specimen exposed to 0.5 wt.% chloride addition. In this case, the surface is non-uniformly attacked: in some places pits are observed (typical “cauliflower” shape appearance), while other zones are free of attack in correspondence with what is observed in Fig. 6c. Fig. 10c shows the specimen exposed to 5 wt.% chloride addition. The surface is heavily pitted. In some cases grain boundaries can be observed inside pits (Fig. 10d).

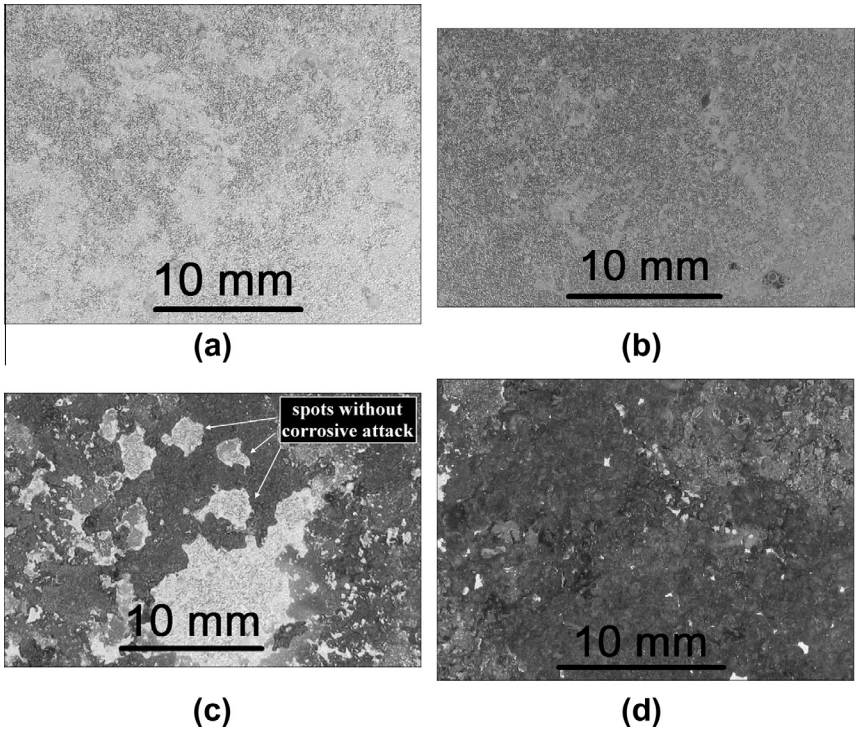

Fig. 6. Optical images of steel plates after tests. (a) No additions; (b) addition of 2.3 wt.% sulphate; (c) addition of 0.5 wt.% chloride, and (d) addition of 5 wt.% chloride.

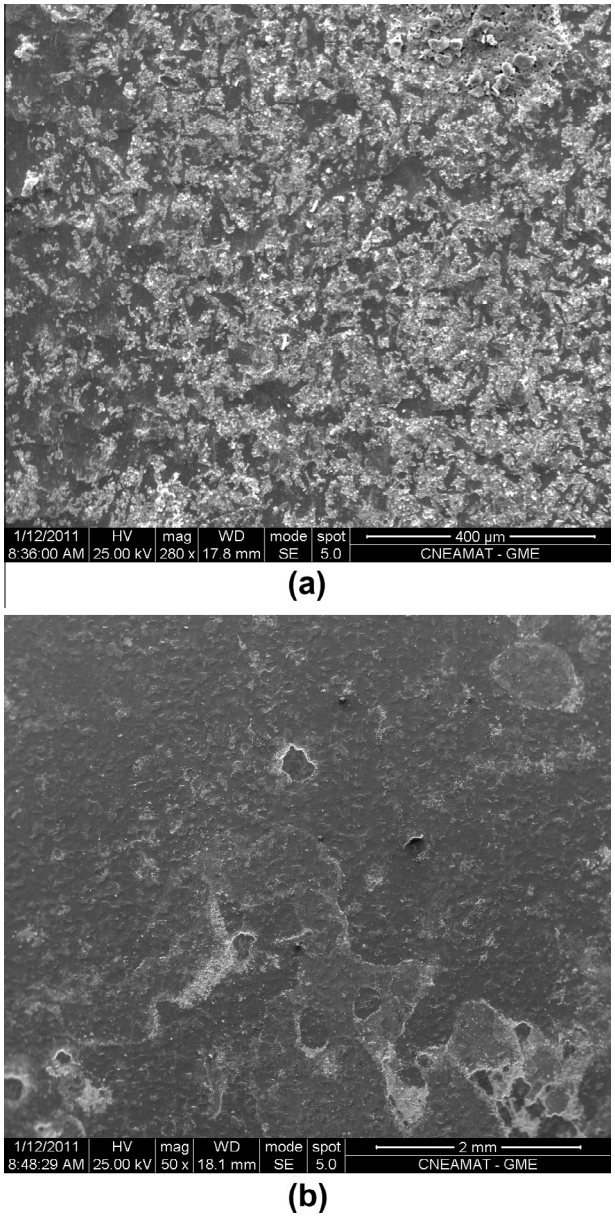

Fig. 7. SEM micrographs of steel plates after tests. (a) No additions; (b) addition of 2.3 wt.% sulphate.

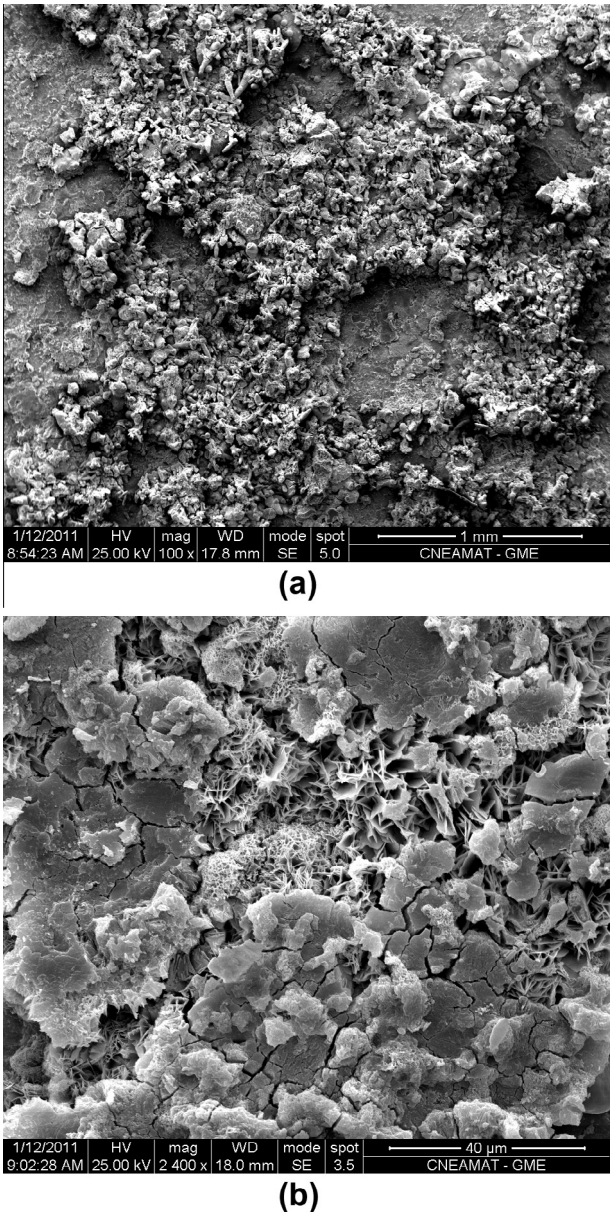

Fig. 8. SEM micrographs of steel plates after tests with the addition of 0.5 wt.% chloride.

Fig. 11 shows metallographic cross sections of the specimens exposed to 5 wt.% chloride addition, before and after the removal of the corrosion products. Both, general attack (Fig. 11a and b) and pitting (Fig. 11c and d) are observed. In the case of non-scaled surfaces, corrosion products of different colours are detected both, when general corrosion occurs and inside pits. To identify these compounds, TMS of the corrosion products was performed at room temperature. The powder was removed from the rust by manual scraping of the steel plates with an acrylic spatula. Fe^{3+} compounds are the majority species (>83%). Reasonable fits were obtained using a distribution of hyperfine fields and 2 doublets (Fig. 12), with the following hyperfine parameters: CI 0.34 mm/s and DC 0.50 mm/s for one doublet; and CI 0.34 mm/s and DC 0.83 mm/s for the other quadruple doublet. These parameters are consistent with paramagnetic akaganeite as the main compound [26]. The distribution of hyperfine fields was attributed to the presence of goethite (by fitting the magnetic part of the spectra with a distribution of hyperfine magnetic fields with maxima around 38 T); magnetite and/or nonstoichiometric maghemite (corresponding to a distribution of hyperfine magnetic fields with maxima around 46 y 49 T), and hematite (hyperfine magnetic fields with maxima around 51 T) [26]. These compounds were found in lower concentrations than akaganeite. SEM photographs from representative locations of the rust samples exposed to 5 wt.% chloride addition (Fig. 9), are in agreement with the findings from Mössbauer analysis. It is known that in a chlorinated matrix, steel corrosion results from depassivation due to chlorides. The passivating products are transformed in non-protective products that, in the presence of oxygen are, mainly, FeOOH (lepidocrocite and akaganeite) [27]. The results obtained in the present work also agree with the above mentioned statement.

At this point it should be mentioned that corrosion rates measured with the linear polarisation resistance technique assume that only uniform attack is occurring at the steel surface. But, from the descaled specimens (Fig. 10b and c) and the metallographic cross-sections (Fig. 11) of steel exposed to 5 wt.% chloride, not only

uniform attack but some type of extended pitting is also observed. These observations would imply that the corrosion rate values obtained with the linear polarisation resistance technique are unsuitable. However, according to González et al. [28], the maximum penetration of localised attack on steel in contact with cement containing chlorides is equivalent to about four to eight times the average general penetration. As a consequence, it is considered that there is not significant error in considering the CR values as though the attack were uniform.

From the metallographic cross sections, the thickness of the remaining steel plate was measured. From these measurements, the depth of the corrosive attack was determined by subtracting these values from the original thickness of the steel plates. For specimens exposed to 5 wt.% chloride addition, the maximum depth of the corrosive attack is 150 μm. Taking into account that the test duration was 900 days, the average corrosion rate at that location is about 60 μm/year. Besides, from Fig. 5, it is evident that the corrosion rate in the case of 5 wt.% chloride addition, is only significant during the first year of exposure. After 1 year, the corrosion rate drops abruptly reaching a value close to 0.1 μm/year. This implies that most of the 150 μm of corrosive attack must have occurred during the first year. When applying these results to estimate if the durability of the steel drums will be higher than the foreseen life span of the facility (300 years), the following computation should be done: the maximum depth of the total corrosive attack would be 150 μm (that would occur during the first year of exposure) plus the corrosion penetration that would occur during most of the rest of the time. Assuming a constant corrosion rate of 0.1 μm/year from the first year of exposure and during most of the life span of the facility, this last contribution would yield about 30 μm. As a consequence, a total corrosion penetration higher than 180 μm is not to be expected. Taking into account that the thickness of the wall of the steel drums is 0.9 mm, it is predicted that the durability of the steel drums will be higher than the foreseen life span of the facility, thereby guaranteeing its durability. It is worth mentioning that these values correspond to the most conservative approach, because calculation were performed for the most concentrated chloride condition.

In order to explain the decrease of the corrosion rate as a function of time in the tests performed with 5 wt.% chloride additions, three possibilities were analysed: the lack of oxygen to sustain the corrosion process after its consumption during the first months; the blockage of the pitting by the corrosion products generated during the first stages of the test; or the lack of water necessary for the corrosion process to occur. If the first possibility were the case (lack of oxygen), very low corrosion potentials should be observed by the time the corrosion rate decreases [29] and, in the present work, it was found that the corrosion potential increases while the corrosion rate decreases. When computing the area under the curves in Fig. 5 to assess the total amount of corrosion in each case, the specimens exposed to a high chloride concentration yields an area that is 2.5 orders of magnitude greater than that corresponding to a low chloride concentration. If oxygen were the limiting species, there is no reason for the corrosion rate with 0.5 wt.% chloride to decrease after about 120 days, when oxygen was still available to sustain even higher corrosion rates at 300 days in the more concentrated chloride condition.

The second possibility assumes that the corrosion products formed on the steel during pitting propagation are compact and that, when accumulating, they partly blocked up the pit mouth, isolating the propagating pit from the matrix and as a consequence the corrosion process stops. But, when observing the morphology

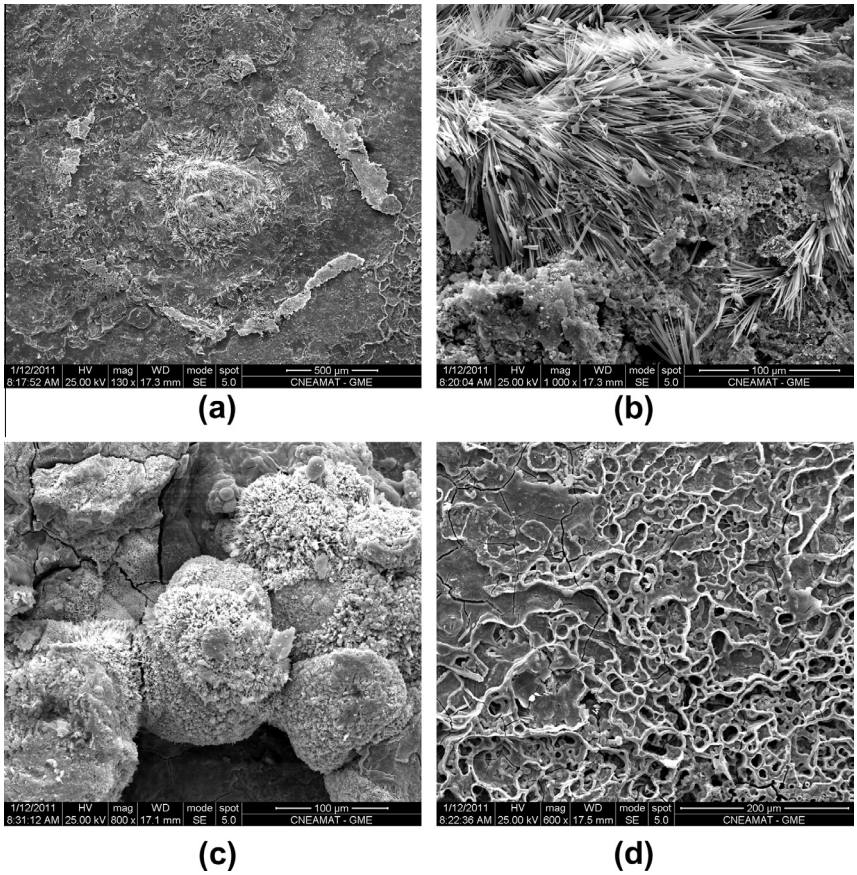

Fig. 9. SEM micrographs of steel plates after tests with the addition of 5 wt.% chloride.

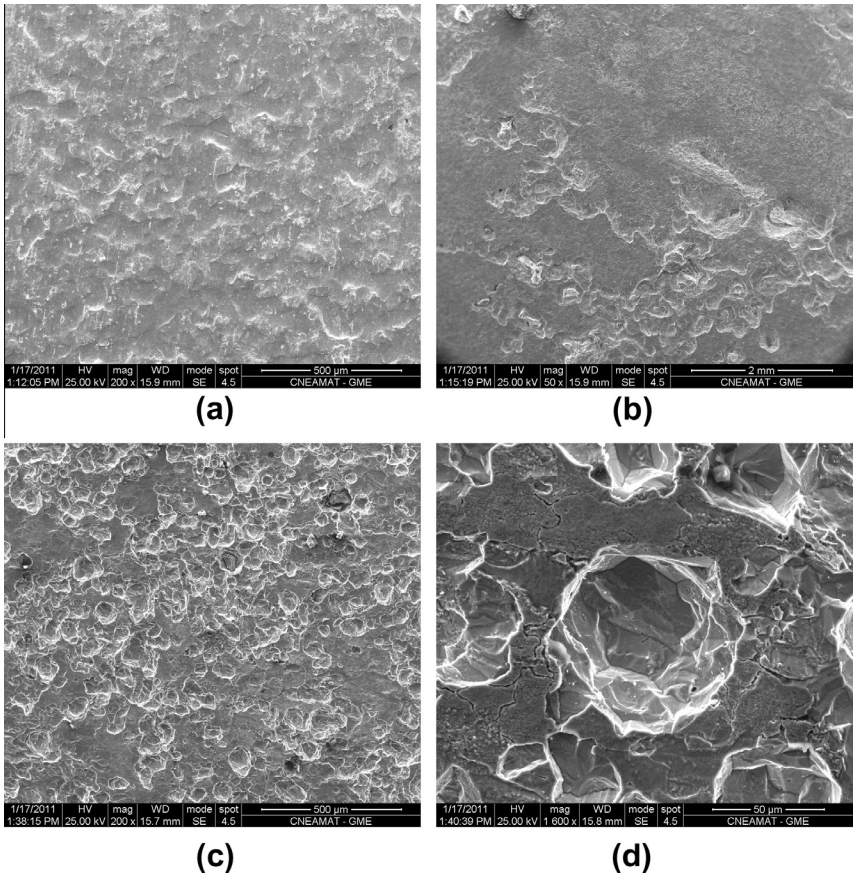

Fig. 10. SEM micrographs of steel plates after descaling. (a) No additions; (b) addition of 0.5 wt.% chloride, (c), and (d) addition of 5 wt.% chloride.

of the corrosive attack (e.g. Figs. 10c and 11b), it can be seen that the pits are extended and with the typical 'cauliflower' shape appearance. This implies that the pitśaspect ratio is low and the possibility of blocking the pit mouth is then discarded.

The third possibility (lack of water) as a cause of the decrease of the corrosion rate, can be validated when the evolution of the electrical resistivity of the matrixes (Fig. 3) is taken into account. No similar systems to that studied in the present work were found in the literature but, the discussion can be based on analogue systems (corrosion of steel in reinforced concrete). Alonso et al. [30] stated that when steel is passivated, the corrosion rate is not affected by resistivity but, when active corrosion is in progress (as it is the case for chloride contaminated specimens), the electrical resistivity of concrete seems to be a factor which controls the corrosion rate. Morris et al. [31] found that reinforcing steel bars are likely to present an active corrosion state when concrete presents a resistivity value lower than approximately 10 kohm cm. On the other hand, the steel reinforcement remains in a passive state when resistivity is higher than approximately 30 kohm cm. Other references are cited by Morris et al. [31], where the threshold resistivity value from the passive to active state of the steel lies between 10 and 65 kohm cm. Aperador et al. [32] found that the corrosion of reinforced bars embedded in a highly carbonated concrete is inhibited due to an electrical resistivity of the matrix higher than 20 kohm cm. Finally, Andrade and Alonso [18] found that when the resistivity of concrete is higher that 100–200 kohm cm, the corrosion rate is negligible due to a very dry matrix. In spite of the differences in the threshold values of the resistivity reported in the literature, there is a general agreement in accepting that concrete resistivity influences the corrosion rate. As can be seen, the limit of the electrical resistivity value above which the corrosion rate is negligible, depends on the experimental conditions. When comparing Figs. 3–5, it can be observed that, for chloride contaminated specimens, when the value of the electrical resistivity is higher than 20 kohm cm, the corrosion rate stars to decrease (at about 120 days for 0.5 wt.% chloride and about 320 days for 5 wt.% chloride). So, this is a strong support to the theory that the decrease in the corrosion rate observed in aggressive conditions is due to the lack of water for sustaining the electrochemical processes. Indeed, when observing the corrosion products in the present work, it is found that they are extremely dry, then the conclusion is that the decrease of the corrosion rate with time, after reaching a high corrosion rate value, is due to the dryness of the matrix that hinders the development of the corrosion process, no matter the high concentration of aggressive species and the presence of oxygen.

As it was mentioned in the introductory section, due to a conservative approach, the steel drums are not considered as physical barriers for the safety analysis, being the concrete the sole barrier to avoid the radionuclide release during the life span of the nuclear waste disposal facility. However, from the results obtained in the present work, an extra safety period is obtained. Besides, it should be mentioned that in the design of the facility it is indicated that drums will be internally coated with some kind of protective paint that would result in an even longer safety period. Anyway, it is not clear what could happen if there is a flaw in the coating and the bare metal is locally exposed to the cemented waste form. In this situation localised corrosion could be a potential threat to the lifetime of the drums because of the presence of aggressive species. Future work performed on steel sheets with a coating locally scratched to exposed the bare metal to the environment should be performed to elucidate this point.

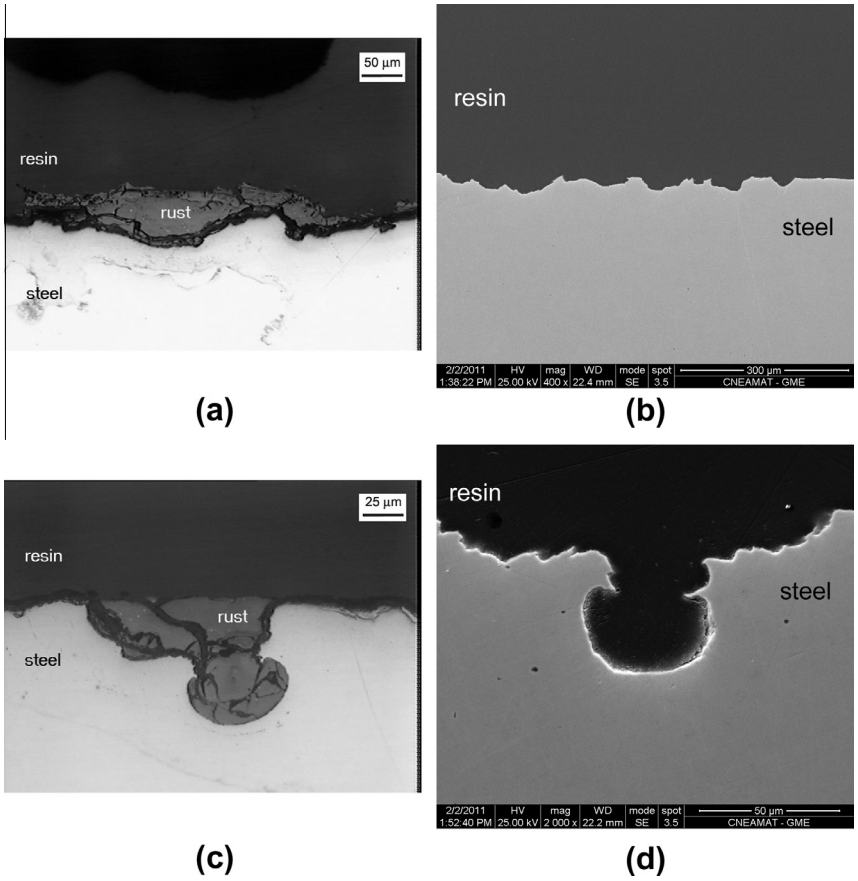

Fig. 11. Different types of attack on steel plates exposed to 5 wt.% chloride, before (left) and after (right) the descaling of the corrosion products: (a) and (b) general corrosion; (c) and (d) pitting corrosion.

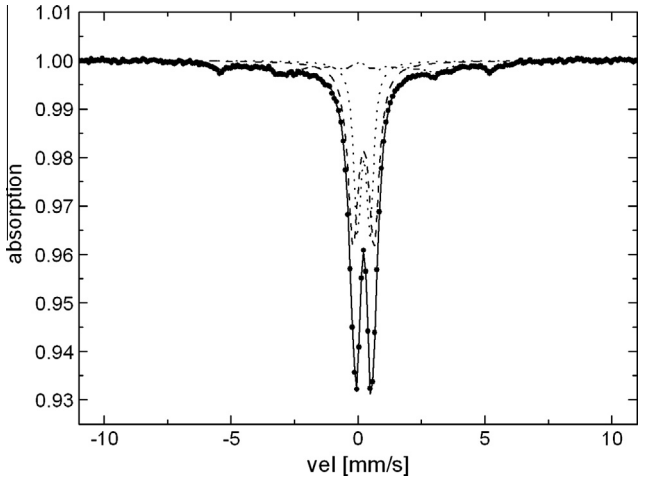

Fig. 12. Mössbauer spectra of corrosion products obtained from steel plates exposed to 5 wt.% chloride addition.

If the present work had been conducted over one year period, the conclusion would have been that the steel drums will be perforated by corrosion in few years. However, it was found that after 1 year of exposure, the corrosion rate decreases significantly leading to a very different conclusion. A very long lifetime is required for the repository (300 years). Prediction for such a long period is very unusual in corrosion technology. For practical reasons, the exposure time will, even in rigorous tests, be restricted to months or years. An extrapolation of the results to hundreds of years will, of course, involve uncertainties. Small errors in the measured corrosion rates may result in misleading conclusions after extrapolation. Further, the corrosion mechanism may change, and even unforeseen corrosion phenomena may appear during the extreme time spans to be considered. These uncertainties are reduced by studying the processes observed on archaeological artefacts [33]. These cultural heritage objects are used as analogues to provide data on the corrosion state in natural environments over long periods, situations that cannot always be simulated by laboratory experiments.

4. Conclusions

From the present work, the following conclusions can be drawn:

(1) The corrosion rate of the steel in contact with cemented ion-exchange resins in the absence of contaminants or in the presence of 2.3 wt.% sulphate content remains low (less than 0.1 µm/year) during the whole period of the study (900 days).
(2) The presence of chloride ions increases the corrosion rate of the steel at the beginning of the exposure but, after 1 year, the corrosion rate drops abruptly reaching a value close to 0.1 µm/year. This is probably due to the lack of water to sustain the corrosion process.
(3) When applying the results obtained in the present work to estimate the corrosion depth of the steel drums containing the cemented radioactive waste after a period of 300 years, it is found that in the most unfavourable case (high chloride contamination), the corrosion penetration will be considerably lower than the thickness of the wall of the steel drums.

(4) Cementation of ion-exchange resins does not seem to pose special risks regarding the corrosion of the steel drums that contained them; even in the case the matrix is highly contaminated with chloride ions.

Acknowledgements

The financial support of the CONICET (Consejo Nacional de Investigaciones Científicas y Técnicas), the Universidad Nacional de San Martín (UNSAM) and of the FONCYT, Secretaría para la Tecnología, la Ciencia y la Innovación Productiva, Argentina, is acknowledged.

References

[1] Joint convention on the safety of spent fuel management and on the safety of radioactive waste management. National Report, Argentina, 2003, <http://www.cab.cnea.gov.ar/residuos/CC2003/0002-SecA.pdf> (accessed 25.03.11).
[2] M.S. Sayed, M.M. Khattab, J. Am. Sci. 6 (2010) 334–341.
[3] N. Stevens, E. Tsausoglou, E. Onumonu, Mechanistic Investigation of Internal Corrosion of Nuclear Waste Containers over Extended Time Periods, Proc. Eurocorr, 2008, paper 1318, Edinburgh.
[4] X. Gan, M. Lin, L. Bao, Y. Zhang, Z. Zhang, J. Nucl. Sci. Technol. 45 (2008) 1084–1090.
[5] F.P. Glasser, Cem. Concr. Res. 22 (1992) 201–216.
[6] J.D. Palmer, G.A. Fairhall, Cem. Concr. Res. 22 (1992) 325–330.
[7] M.L.D. Gougar, B.E. Scheetz, D.M. Roy, Waste Manage. 16 (1996) 295–303.
[8] J.M. Ducoulombier, B. Lantes, M. Bordier, Nucl. Eng. Des. 176 (1997) 27–34.
[9] I. Plecas, R. Pavlovic, S. Pavlovic, Leaching behaviour of 60Co and 137Cs from spent ion exchange resins in cement–bentonite clay matrix, J. Nucl. Mater. 327 (2004) 171–174.
[10] J. Li, G. Zhao, J. Wang, Nucl. Eng. Des. 235 (2005) 817–820.
[11] J. Li, J. Wang, J. Hazard. Mater. B135 (2006) 443–448.
[12] G.S. Duffó, S.B. Farina, F.M. Schulz, F. Marotta, J. Nucl. Mater. 405 (2010) 274–279.
[13] F. Frizon, C. Cau-dit-Caumes, J. Nucl. Mater. 359 (2006) 162–173.
[14] G.S. Duffó, S.B. Farina, C.M. Giordano, Electrochim. Acta 54 (2009) 1010–1020.
[15] G.S. Duffó, S.B. Farina, C.M. Giordano, Mater. Corros. 61 (2010) 480–489.
[16] C. Andrade, J.A. González, Werkst. Korros. 29 (1978) 515–519.
[17] R.A. Brandt, Normos Program, Julich, Forschungszentrum Julich GmbH (KFA), Germany, 1989.
[18] C. Andrade, M.C. Alonso, Constr. Build. Mater. 15 (2001) 141–145.
[19] ASTM C 0876-91R99, Test method for half-cell potential for uncoated reinforcing steel in concrete, American Society of Testing and Materials, Philadelphia, 2004.
[20] C. Andrade, M.C. Alonso, J.S. Gonzalez, An initial effort to use the corrosion rate measurements for estimating rebar durability, in: N.S. Berke, V. Chaker, W.D. Whiting (Eds.), Corrosion Rates of Steel in Concrete, ASTM STP 1065, ASTM International, Philadelphia, 1990, pp. 29–37.
[21] C. Andrade, C. Alonso, Constr. Build. Mater. 15 (1996) 315–328.
[22] D. de la Fuente, I. Díaz, J. Simancas, B. Chico, M. Morcillo, Corros. Sci. 53 (2011) 604–617.
[23] D.A. Koleva, J. Hu, A.L.A. Fraaij, P. Stroeven, N. Boshkov, J.H.W. de Wit, Corros. Sci. 48 (2006) 4001–4019.
[24] A. Raman, S. Nasrazadani, L. Sharma, Metallography 22 (1989) 79–96.
[25] A. Razvan, A. Raman, Pract. Metallogr. 23 (1986) 223–236.
[26] E. Murad, J.H. Johnston, Iron oxides and oxyhydroxides, in: G. Long (Ed.), Mössbauer Spectroscopy Applied to Inorganic Chemistry, vol. 2, Plenum Publ. Corp., New York, 1987, pp. 507–589.
[27] M. Pourbaix, Corros. Sci. 30 (1990) 963–988.
[28] J.A. González, C. Andrade, C. Alonso, S. Feliu, Cem. Concr. Res. 25 (1995) 257–264.
[29] M. Raupach, Mater. Struct. 29 (1996) 174–184.
[30] C. Alonso, C. Andrade, J.A. Gonzalez, Cem. Concr. Res. 8 (1988) 687–698.
[31] W. Morris, A. Vico, M. Vazquez, S.R. de Sanchez, Corros. Sci. 44 (2002) 81–99.
[32] W. Aperador, R. Mejías de Gutierrez, D.M. Bastidas, Corros. Sci. 51 (2009) 2027–2033.
[33] D. Neff, M. Saheb, J. Monnier, S. Perrin, M. Descostes, V. L'Hostis, D. Crusset, A. Millard, P. Dillmann, J. Nucl. Mater. 402 (2010) 196–205.